CONTRIBUTION FROM THE DEPARTMENT OF CHEMICAL ENGINEERING,
UNIVERSITY OF TEXAS, AUSTIN, TEXAS

The Phase Equilibria and Crystal Chemistry of the Intermediate Phases in the Ytterbium–Antimony System[1]

BY R. E. BODNAR AND H. STEINFINK

Received September 9, 1966

Seven stable intermediate phases have been found to exist in the ytterbium–antimony system. $YbSb_2$ is orthorhombic, Cmcm, and is isostructural with $ZrSi_2$; YbSb is fcc and has the NaCl structure with a = 6.082 A; two phases having the 5:4 stoichiometry exist with the $\alpha \rightarrow \beta$ transition occurring at 1030°. The low-temperature form, α-Yb_5Sb_4, is tetragonal, $I^4/_m$mm, with a = 11.90 A and c = 17.06 A. The high-temperature form, β-Yb_5Sb_4 is orthorhombic, Pnma or $Pn2_1a$, with a = 8.13 A, b = 15.97 A, and c = 24.39 A. The phase Yb_4Sb_3 is bcc, $I\bar{4}3d$, with a = 9.320 A, and has the *anti*-thorium phosphide, Th_3P_4, structure. The alloy Yb_5Sb_3 is hexagonal, $P^6/_m$cm, with a = 8.995 A and c = 6.870 A and is isostructural with Mn_5Si_3. The phase richest in ytterbium is Yb_5Sb_2, orthorhombic, $Pn2_1a$, with a = 12.32 A, b = 9.60 A, and c = 8.32 A. Two phases, $YbSb_2$ and Yb_4Sb_3, melt congruently at 945 and 1540°, respectively. The β form of Yb_5Sb_4 melts incongruently at 1400° while YbSb decomposes at 820°. The remaining phases, Yb_5Sb_3 and Yb_5Sb_2, melt incongruently at 1520 and 1400°, respectively, but loss of ytterbium vapor occurs at the melting point indicating vapor–solid equilibrium in this region of the phase diagram.

Introduction

Ytterbium displays divalent and trivalent oxidation states in its compounds and similar behavior can be expected to occur in intermediate phases formed between it and semimetals such as antimony and bismuth. McMasters and Gschneidner[2] investigated the Yb–Mg system and found that ytterbium displays divalent character throughout the diagram. The intermediate phase YbSb has been reported by Iandelli[3] and Brixner,[4] and the phases YbSe and YbTe have been reported by Senff and Klemm;[5] all of these are isostructural with NaCl. As part of a program dealing with the study of rare earth–group Va and VIa systems, the phase diagram, crystal chemistry, and magnetic susceptibility of the intermediate phases found in the Yb–Sb system have been investigated in order to determine whether the oxidation state of the rare earth atom varies in these alloys and what, if any, correlation exists between observed bond lengths in the different phases and their magnetic moments. This paper discusses the phase diagram and crystal chemistry of the system and the results of the magnetic measurements and discussion of the oxidation states of ytterbium will be published elsewhere.

Experimental Section

Ytterbium metal of 99.9% purity was obtained from the Nuclear Corp. of America and antimony of 99.99% purity was obtained from Johnson, Mathey and Co. Samples of appropriate composition of the elements were sealed in tantalum tubes under several millimeters of argon and allowed to react. The lower melting phases $YbSb_2$, YbSb, and α-Yb_5Sb_4 were prepared by heating at 800° for 3–4 days in conventional resistance furnaces capable of reaching 1200° and holding at ±5°. In this procedure the tantalum ampoules were again sealed into large Vycor tubes to prevent oxidation of the tantalum tubes. Quenching of samples from the resistance furnaces was accomplished by dropping the tubes into ice water or brine. Quenching times of 2–5 sec were obtained. Intermediate phases with higher melting points (β-Yb_5Sb_4, Yb_4Sb_3, Yb_5Sb_3, and Yb_5Sb_2) were allowed to react for shorter periods to reduce the reaction of antimony with tantalum. Reaction times of 2–5 min in a vacuum induction furnace at 1100–1600° were found to be satisfactory. Quenching in the induction furnace was not as rapid since there was no means to remove heat suddenly. However, temperature drops of 1000° could be obtained in less than 1 min. All sample annealing was done in tantalum tubing at temperatures approximating 75% of the melting points.

Single-crystal and powder X-ray diffraction techniques were used to identify the phases. Microscopic examination was also used to determine the nature of the quenched samples. Density measurements were made by the displacement technique using acetone as the liquid. Melting points were measured by a procedure previously described.[6]

Single-crystal X-ray diffraction data were collected for $YbSb_2$, Yb_4Sb_3, and Yb_5Sb_3 to confirm the crystal structures and to obtain more accurate values for the bond distances. Small crystals of irregular shape were selected for each phase. No absorption corrections were applied and isotropic temperature factors were used in all instances. Crystal structure determinations are now in progress on the intermediate phases whose structures are unknown.

Results

Phase Diagram.—A proposed equilibrium phase diagram for the Yb–Sb system is presented in Figure 1. Solid lines represent regions elucidated by a study of quenched samples and the dashed lines represent uncertain areas. The symbols denote observations made on quenched samples. No efforts were made to determine the eutectic points precisely, nor was the solubility at the terminal ends of the diagram studied.

The study of this binary system was complicated by the extreme volatility of the ytterbium metal. Large pressures were developed inside the tantalum tubes during the reaction, and these made pressure an active thermodynamic variable. Except for Yb_5Sb_3, the reaction pressures were probably less than 1 atm at reaction temperatures near 1000°. The pressures de-

---

(1) Research sponsored by National Science Foundation Grant GP-2029.

(2) O. D. McMasters and K. A. Gschneidner, *J. Less-Common Metals*, **8**, 289 (1965).

(3) A. Iandelli, "Rare Earth Research," The Macmillan Co., New York, N. Y., 1961.

(4) L. H. Brixner, *J. Inorg. Nucl. Chem.*, **15**, 199 (1960).

(5) H. Senff and W. Klemm, *Z. Anorg. Allgem. Chem.*, **242**, 92 (1939).

(6) D. J. Haase, H. Steinfink, and E. J. Weiss, *Inorg. Chem.*, **4**, 541 (1965).

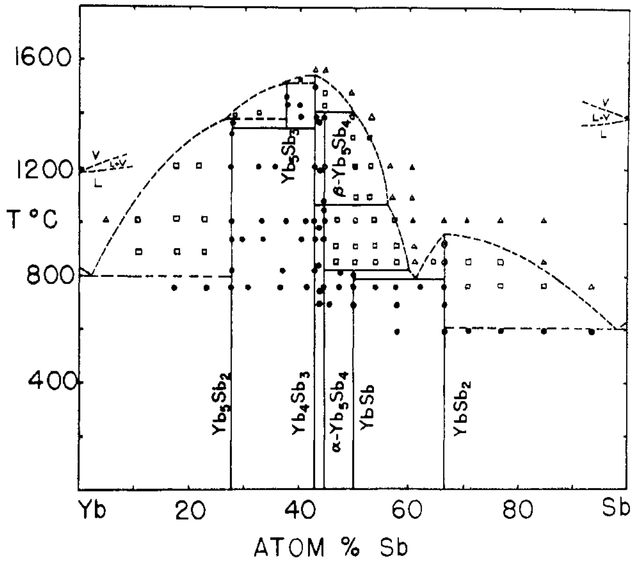

Figure 1.—Proposed phase diagram for the system Yb–Sb: O, single-phase solid; ●, two-phase solid; □, liquid and solid; △, liquid.

veloped in producing Yb_5Sb_3 around 1400° were more than 1 atm as evidenced by the bulging of the tantalum reaction containers. Since the boiling points of the elements are quite low, they are included on the diagram along with the initial portion of the liquid–vapor loop for both elements. A linear behavior would lead to the intersection of the vapor–liquid loop with the liquid–solid region resulting in vapor–solid equilibrium. Sublimation rather than melting of Yb_5Sb_2 and Yb_5Sb_3 was observed when their melting points were determined.

Further difficulty was encountered because of a violent exothermic reaction which occurred near 600° as the sample containers were heated to the normal reaction temperatures. This behavior dispersed the elemental constituents on the walls of the container and thereby prevented the establishment of equilibrium conditions. This effect was reduced significantly by compacting the reaction mixtures into pellets and also by heating very slowly across this temperature range.

X-Ray diffraction powder patterns of quenched samples richer in Sb than 66.7 atom % showed $YbSb_2$ and Sb in equilibrium. $YbSb_2$ was found to melt congruently at 845 ± 15°. Samples with Sb compositions between 50 and 66.7 atom % which had reacted below 800° showed that YbSb and $YbSb_2$ were in equilibrium. Quenched samples between 820 and 1130° showed no sign of YbSb, but a mixture of liquid and either α-Yb_5Sb_4 or $YbSb_2$, depending on the composition. Samples near 60 atom % Sb when slow-cooled across the 800° isotherm showed YbSb and $YbSb_2$ in approximately a 2:1 ratio, indicating a eutectic point near 60%. The α-Yb_5Sb_4 composition was obtained at 44.4 atom % Sb, and samples with slightly less antimony showed α-Yb_5Sb_4 and Yb_4Sb_3 in equilibrium below 1030° and those with slightly more antimony showed α-Yb_5Sb_4 and YbSb in equilibrium below 820°; transformation to β-Yb_5Sb_4 occurred above 1030°. The phase β-Yb_5Sb_4 could also be produced from the elements in the correct proportion above 1030° and it melted incongruently at 1400 ± 25°.

The phase Yb_4Sb_3 was produced at temperatures ranging from 800 to 1400° although the optimum condition for synthesis was near 1000°. It melts congruently at 1540 ± 10° and the vapors leaving the molten liquid when condensed on a cold glass slide were still of the same structure and composition as the original solid. The compound Yb_5Sb_3 was produced at temperatures above 1350° and appeared to exist in equilibrium with Yb vapor. At 1520 ± 10°, loss of Yb resulted in the formation of Yb_4Sb_3. Specimens of Yb_5Sb_3 were stable at room temperature but when heated above 1100° would dissociate to Yb_4Sb_3 and Yb_5Sb_2. It was impossible to produce homogeneous samples of Yb_5Sb_3 below 1350°.

The best single-phase material of the phase richest in Yb was at the 28.6 atom % Sb composition. It could be produced at temperatures ranging from 825 to 1300° although loss of Yb from volatilization was more serious at elevated temperatures. The phase Yb_5Sb_2 releases Yb vapors when heated in open containers above 1000°, and at 1400° it is completely dissociated. From density and volume considerations, each unit cell contains 30 atoms, but at a 5:2 composition, this would imply partial atom occupancy. It is possible that a range of homogeneity exists for this phase, but no attempt was made in the present work to determine composition variability.

The element Yb is normally face-centered cubic and has a phase transition to body-centered cubic at 720°. We have also observed a phase transition to a hexagonal close-packed structure which was stable above 300° and thus ytterbium also displays the structure in which all the other rare earth elements in the latter half of the series crystallize. The lattice parameters a = 3.855 A and c = 6.280 A are consistent with the size anomaly usually encountered with Yb. The hexagonal form has also been reported by Spedding, *et al.*,[7] who considered it an impurity-stabilized phase, where the contaminant is oxygen or nitrogen, and by Stephens,[8] who reports its presence in Yb which was at least 99.86 wt % pure.

Crystal Data

The crystallographic and physical parameters are summarized in Table I; X-ray powder diffraction data are shown in Table II. Lattice constants for $YbSb_2$, YbSb, Yb_4Sb_3, and Yb_5Sb_3 were obtained by measurements of powder diffraction lines in the back-reflection region and plotting those values against $\sin^2 \theta$. Extrapolation to $\sin^2 \theta = 1$ yielded the values shown in Table I and they are considered accurate to ±0.002 A. The other phases had powder patterns that were too complex and the lines in the back reflection region cannot be indexed unambiguously; the lattice constants for these phases are accurate to ±0.01 A.

---

(7) F. H. Spedding, J. J. Hanak, and A. H. Daane, *J. Less-Common Metals*, **3**, 110 (1961).

(8) D. R. Stephens, *Phys. Chem. Solids*, **26**, 943 (1965).

TABLE I

CRYSTAL CHEMISTRY OF THE Yb–Sb INTERMEDIATE PHASES

Phase	Unit cell constants, A	Space group	Structure type	Unit cell vol., A³	No. of atoms per unit cell	Density, g/cm³ Obsd	Density, g/cm³ X-Ray	Mp,[a] °C
$YbSb_2$	$a = 4.536$	Cmcm	$ZrSi_2$	322.2	12	8.28	8.58	945
	$b = 16.63$							C
	$c = 4.271$							
YbSb	$a = 6.082$	Fm3m	NaCl	225.0	8	8.48	8.71	820
								I
α-Yb_5Sb_4	$a = 11.90$	$I^4/_mmm$	. . .	2415.9	~86	7.63	8.88	1030
	$c = 17.06$							$\alpha \rightarrow \beta$
β-Yb_5Sb_4	$a = 8.13$	Pnma		3166.7	108	8.31	8.51	1400
	$b = 15.97$	or	. . .					I
	$c = 24.39$	$Pn2_1a$						
Yb_4Sb_3	$a = 9.320$	$I\bar{4}3d$	Th_3P_4	809.6	28	8.56	8.67	1540
								C
Yb_5Sb_3	$a = 8.995$	$P^6/_mcm$	Mn_5Si_3	481.4	16	8.10	8.48	1520
	$c = 6.870$							S
Yb_5Sb_2	$a = 12.32$							
	$b = 9.60$	$Pn2_1a$	. . .	984.0	30	7.88	8.03	1400
	$c = 8.32$							S

[a] C denotes congruent melting, I denotes incongruent melting, and S denotes sublimation.

TABLE II

X-RAY POWDER DIFFRACTION DATA FOR THE Yb–Sb INTERMEDIATE PHASES

$YbSb_2$

$d_{obs.}$ Å	$d_{calc.}$ Å	hkl	Intensity*
3.798	3.799	021	10
3.509	3.511	130	12
2.980	2.979	041	8
2.779	2.772	060	25
2.716	2.712	131	100
2.330	2.325	061	10
2.273	2.268	151, 200	15
2.130	2.135	002	15
1.955	1.947	221	2
1.872	1.869	081, 171	5
1.823	1.824	132	5
1.763	1.755	260	12
1.719	1.711	190	8
1.692	1.692	062	8
1.671	1.671	152	5
1.596	1.589	191	8
1.566	1.556	202	12
1.386	1.381	0120	10
1.356	1.347	043	8
1.340	1.335	192	7
1.318	1.318	012,1	10
**			

YbSb

$d_{obs.}$ Å	$d_{calc.}$ Å	hkl	Intensity*
4.512	3.512	111	3
3.036	3.041	200	100
2.148	2.150	220	85
1.834	1.834	311	2
1.754	1.755	222	22
1.518	1.520	400	26
1.390	1.395	331	2
1.358	1.360	420	50
1.241	1.241	422	20
1.170	1.170	333, 511	1
1.075	1.075	440	10
1.028	1.028	531	1
1.013	1.013	422, 600	20
0.961	.961	620	15
0.927	.927	533	<1
0.916	.916	622	10

Yb_4Sb_3

$d_{obs.}$ Å	$d_{calc.}$ Å	hkl	Intensity*
3.799	3.805	211	10
3.285	3.295	220	7
2.936	2.947	310	100
2.483	2.481	321	70
2.079	2.084	420	14
1.984	1.987	332	12
1.899	1.902	422	26
1.825	1.828	431, 510	23
1.510	1.512	532, 611	26
1.472	1.473	620	14
1.436	1.438	541	16
1.373	1.374	631	7
1.343	1.345	444	9
1.287	1.268	552, 633, 712	14
1.244	1.245	642	7
1.182	1.183	651, 732	8
1.113	1.114	653	5
1.098	1.098	660, 822	6
1.083	1.083	743, 750, 831	10

All patterns were obtained with nickel filtered copper radiation

α-Yb_5Sb_4

$d_{obs.}$ Å	$d_{calc.}$ Å	hkl	Intensity*
3.278	3.285	105	5
3.234	3.240	321	5
2.995	2.998	224	15
2.972	2.975	400	35
2.873	2.876	215	90
2.846	2.848	006	100
2.819	2.824	314	50
2.798	2.800	330	95
2.688	2.687	116	15
2.657	2.659	332	25
2.582	2.589	305	60
2.568	2.574	413	25
2.533	2.540	422	5
2.442	2.441	404	15
2.372	2.374	325	5
2.345	2.357	431, 501	5
2.199	2.205	415	25
2.102	2.103	440	10
2.056	2.060	523	5
2.043	2.048	514	12
2.009	2.010	208	8
1.996	1.998	336	10
1.981	1.983	600	30
1.952	1.953	505, 435	8
1.932	1.932	602	5
1.905	1.905	228	5
1.865	1.864	417	5
1.851	1.856	525	30
	1.850	613	
1.846	1.846	541	10
1.804	1.805	516	10
1.789	1.788	219	5
1.766	1.767	543	12
1.735	1.735	408	10
1.710	1.709	00, 10	10
1.693	1.698	615	12
	1.692	701	
1.663	1.666	428	5
1.649	1.650	712, 562	5
**			

β-Yb_5Sb_4

$d_{obs.}$ Å	$d_{calc.}$ Å	hkl	Intensity*
4.073	4.065	200	3
3.645	2.635	203	10
3.550	2.545	213	5
3.311	2.308	223	15
3.005	3.001	135	90
2.952	2.948	151	5
2.889	2.885	152	30
2.850	2.846	046	40
	2.847	240	
	2.853	234	
2.799	2.809	118	15
2.777	2.772	242	70
2.663	2.658	060	35
2.569	2.571	303	10
2.554	2.552	321	100
2.122	2.118	173	10
2.013	2.016	14, 10	20
2.004	2.005	402	10
1.990	1.994	080	12
	1.989	412	
1.963	1.969	02, 12	10
1.930	1.931	273	5
	1.928	404	
1.859	1.863	415	10
	1.857	177	
1.826	1.826	425	12
1.733	1.736	444	5
1.711	1.714	450	14
1.652	1.650	454	5
1.584	1.595	010, 0	10
	1.592	382	
1.489	1.485	210, 0	15
**			

Yb_5Sb_3

$d_{obs.}$ Å	$d_{calc.}$ Å	hkl	Intensity*
7.778	7.788	100	12
3.889	3.895	200	12
3.455	3.435	002	30
3.151	3.143	102	27
2.938	2.944	210	50
2.737	2.739	112	80
2.702	2.706	211	100
2.589	2.596	300	60
2.581	2.576	202	30
2.155	2.160	310	7
2.133	2.137	221	7
2.057	2.061	311	18
1.881	1.881	222	25
1.812	1.808	213	25
1.726	1.729	321	12
1.693	1.698	410	18
**			

Yb_5Sb_2

$d_{obs.}$ Å	$d_{calc.}$ Å	hkl	Intensity*
3.704	3.683	301	5
3.453	3.447	202	18
3.087	3.080	400	25
3.049	3.046	122	75
2.986	2.987	031	15
2.930	2.922	302	70
2.893	2.888	401	60
2.846	2.840	230	5
2.798	2.800	222	100
2.783	2.796	312	8
2.704	2.706	103	25
2.605	2.604	113	15
2.583	2.592	420	30
2.526	2.529	203	10
2.496	2.496	322	5
2.480	2.475	421	8
2.447	2.445	213	20
2.400	2.401	040	35
2.354	2.357	123	25
2.230	2.219	430	15
2.159	2.158	241, 332	5
2.125	2.120	502	10
2.047	2.051	104	10
2.017	2.015	413	5
1.985	1.993	601	5
1.970	1.970	204	10
1.901	1.893	440	6
1.868	1.867	333	5
1.859	1.856	304	20
1.851	1.850	151	20
1.842	1.841	602	20
1.796	1.809	513	10
1.782	1.790	251	16
1.763	1.767	532	10
1.738	1.740	324	5
1.724	1.723	442	20
1.633	1.629	450	15
1.557	1.560	640	18
**			

*Peak intensities, based on the largest set equal to 100

**Due to the large cell dimensions, many different indices can be assigned to the succeeding lines and the resulting ambiguity makes it pointless to list them

$YbSb_2$.—This phase can be easily identified by its metallic luster and pronounced layered structure. It crystallizes in space group Cmcm and is isostructural with $ZrSi_2$. A discussion of coordination and bond distances as determined from a single-crystal X-ray diffraction investigation has been reported previously.[9]

YbSb.—This phase is produced in the form of a coarse, dark brown powder and crystallizes in the NaCl structure. X-Ray diffraction patterns of quenched YbSb powder samples showed a primitive cubic unit cell, 3.041 A on a side, which may be due to a disordered fcc structure where the atoms are randomly distributed over the Yb and Sb sites. X-Ray patterns of annealed powders and single crystals showed lines corresponding to a fcc structure, confirming the ordered, NaCl-type arrangement of atoms at equilibrium. The Yb–Sb atom separation in this phase is 3.041 A, in good agreement with other rare earth antimonides.

α-Yb_5Sb_4.—This phase crystallizes in a body-centered tetragonal structure and the diffraction symmetry is consistent with one of the space groups $I^4/_mmm$, $I\bar{4}m2$, or I42. On comparison of lattice parameters and extinctions, it appears this phase is isostructural with some monogermanides reported by Tharp, Smith, and Johnson[10] for the latter half of the lanthanide series. Although it is certain this phase is close to a 5:4 stoichiometry, it may have a narrow range of homogeneity, particularly with such a large unit cell. The measured density for this phase, Table I, is considerably lower than the measured values for the other phases. The value 7.63 g/cm³ places 8 formula weights in the unit cell and the average atomic volume would be 33.5 A³ in this phase, deviating grossly from an otherwise smooth plot of mean atomic volume per atom against composition for this system. The material produced by the direct reaction of the elements as well as that produced from the inversion of the high-temperature phase had a spongy appearance and the low value of the density is most likely due to a large number of voids in the ingots. The supposition that approximately 86 atoms are present in the unit cell is based on a value of the mean atomic volume obtained from a plot of mean atomic volume *vs.* atom % Sb. The correct composition will have to await the elucidation of the crystal structure.

β-Yb_5Sb_4.—Single-crystal X-ray patterns of this phase can be indexed on the basis of an orthorhombic cell with space group Pnma or $Pn2_1a$. Smith, John-

---

[9] R. Wang, R. Bodnar, and H. Steinfink, *Inorg. Chem.*, **5**, 1468 (1966).

[10] A. G. Tharp, G. S. Smith, and Q. Johnson, *Acta Cryst.*, **20**, 583 (1966).

son, and Tharp[11] report Sm_5Ge_4 with similar space group and cell constants. The cell constants for β-Yb_5Sb_4 are a = 8.13 A, b = 15.97 A, and c = 24.39 A. The c parameter appears to be 8.13 A, but close examination of X-ray photographs reveals faint reflections which can be attributed to a supercell made by tripling the original c parameter of 8.13 A. This was not observed for Sm_5Ge_4, but might be related in this case to the mechanism of the phase transformation from α-Yb_5Sb_4 to β-Yb_5Sb_4. This supercell was observed on crystals obtained both by direct synthesis of the elements and by the phase transformation from α-Yb_5Sb_4. The crystal structure of this phase is currently under investigation.

Yb_4Sb_3.—This phase crystallizes in the *anti*-thorium phosphide, Th_3P_4, structure. Similar *anti*-Th_3P_4 structures have been reported by Holtzberg[12] and Hohnke and Parthe[13] for 4:3 composition of lanthanides with group IV and V elements. The Th_3P_4 structure is characterized by one variable positional parameter in the space group $I\bar{4}3d$, associated in this case with the Yb atoms. The least-squares refinement of 36 general *hkl* reflections obtained photographically with Mo Kα radiation yielded a value of 0.074 ± 0.001 for the positional parameter. Ideal atomic packing would result in a parameter of 0.083, but the presence of both covalent and ionic bonding displaces the Yb atoms from the ideal position. A value of 0.0745 was obtained by Cox, *et al.*,[14] for La_2Te_3, and Holtzberg, *et al.*,[15] report a positional parameter of 0.0715 for Gd_2Se_3 and 0.075 for La_3Se_4. The compounds Gd_2Se_3 and La_2Te_3 contain vacancies whereas La_3Te_4 does not. The Yb–Sb bond distances in Yb_4Sb_3 are 3.139 and 3.323 A, the two separations resulting from the displacement of the Yb atom from the idealized position. No variation in stoichiometry commonly observed for the regular Th_3P_4-type structure was observed for Yb_4Sb_3.

Yb_5Sb_3.—This phase crystallizes with the manganese silicide, Mn_5Si_3, structure, $D8_8$ type. The variable atomic positions obtained by a least-squares refinement of 70 *hk*0 and *h*0*l* reflections obtained photographically with Cu Kα radiation are shown in Table III.

Table III

Atom	x	$\sigma(x)$	y	z
4-Yb(I)	0.333	...	0.667	0
6-Yb(II)	0.2516	0.0010	0	0.250
6-Sb	0.6115	0.0016	0	0.250

The Yb(I)–Sb bond distances are 3.272 A for the nearly octahedral Sb coordination around the Yb(I) atoms at a fixed position. Two of the Yb(II)–Sb bond distances are 3.240 A, and the third is 3.068 A. This short distance is probably due to the very anisotropic coordination of Yb(II) by the antimony atoms. The sublimation of ytterbium from Yb_5Sb_3 at elevated temperatures is probably due to the loss of Yb(II) atoms which are clustered at the corners of the unit cell.

The Mn_5Si_3 structure has been reported for stannides and plumbides of all of the lanthanides except europium and ytterbium by Jeitschko and Parthe.[16] It appears that the structure is influenced by the number of valence electrons present, and the shortage for Yb is overcome by a trivalent element such as antimony. No other rare earth–group V 5:3 alloys have been reported, and the narrow temperature range may indicate that this phase is not very stable.

Yb_5Sb_2.—This phase is richest in ytterbium and crystallizes in an orthorhombic structure with the probable space group $Pn2_1a$. A crystal structure determination has been undertaken and a proposed structure has been reported.[17] There appear to be atoms with statistical occupancy in the unit cell, and this agrees with the partial atom occupancy referred to earlier.

Discussion

There are seven stable intermediate phases in the system, some of which are isotypic with known structures and others have new structures. $YbSb_2$ appears to be the first $ZrSi_2$-type structure in these rare earth–intermetallic systems. The NaCl structure for YbSb is typical of all of the equimolar group V and VI lanthanides. The *anti*-Th_3P_4 structure for Yb_4Sb_3 has been previously reported for other group V–rare earth alloys of this composition, but the variable position parameter of 0.074 is less than the idealized parameters of $^1/_{12}$ or 0.083. New structures also exist for α-Yb_5Sb_4, β-Yb_5Sb_4, and Yb_5Sb_2. Yb_5Sb_3 appears to be the first Mn_5Si_3 structure reported for a rare earth–group V alloy.

The only other rare earth–antimony system reported is the La–Sb system investigated by Vogel and Klose.[18] Although no crystal structures are given, the phases $LaSb_2$, LaSb, Lab_3Sb_2, and La_2Sb are reported. Since then, Hohnke and Parthe[13] report La_4Sb_3 with the *anti*-Th_3P_4 structure. $LaSb_2$ has been reported by Wang[19] to have a new structure closely related to $YbSb_2$. The La_2Sb structure is probably related to Yb_5Sb_2, but has not been confirmed.

Ytterbium, with the dual oxidation state, exhibits the size anomaly associated with the divalent state for Yb_4Sb_3 when compared to other RE_4Sb_3 alloys. The lack of anomalous behavior for YbSb suggests trivalent Yb behavior in this alloy and this has been reported by Iandelli.[3]

---

(11) G. S. Smith, Q. Johnson, and A. G. Tharp, Abstracts, American Crystallographic Association Meeting, Austin, Texas, 1966.

(12) F. Holtzberg, S. Methfessel, and J. C. Suits, "Rare Earth Research II," K. S. Vorres, Ed., Gordon and Breach, New York, N. Y., 1964.

(13) D. Hohnke and E. Parthe, *Acta Cryst.*, **21**, 435 (1966).

(14) W. L. Cox, H. Steinfink, and W. F. Bradley, *Inorg. Chem.*, **5**, 318 (1966).

(15) F. Holtzberg, Y. Okaya, and N. Stemple, Abstracts, American Crystallographic Association Meeting, Galinburg, Tenn., 1965.

(16) W. Jeitschko and E. Parthe, *Acta Cryst.*, **19**, 275 (1965).

(17) A. Raman and H. Steinfink, Abstracts, Seventh International Crystallographic Union Meeting, Moscow, 1966.

(18) R. Vogel and H. Klose, *Z. Metallkunde*, **45**, 633 (1954).

(19) R. Wang, Ph.D. Dissertation, University of Texas, 1966.